polymers

MDPI

Article

Geant4 Simulation of Photon- and Neutron-Shielding Capabilities of Biopolymer Blends of Poly(lactic acid) and Poly(hydroxybutyrate)

Hanan Akhdar * and Maryam Alshehri

Department of Physics, Faculty of Science, Imam Mohammad Ibn Saud Islamic University (IMSIU), P.O. Box 90950, Riyadh 11623, Saudi Arabia; mfalshehri@imamu.edu.sa
* Correspondence: hfakdar@imamu.edu.sa

Abstract: Simulation is used by scientists to imitate a real-life experimental setup in order to save time, costs and effort. Geant4, a toolkit based on the Monte Carlo method, has been widely used in investigating the radiation-shielding properties of different materials. In many recent studies, researchers have focused on polymers and their shielding capabilities. Poly(lactic acid) (PLA) is a widely used biopolymer in many applications due to its excellent mechanical properties. However, it has limitations related to its degree of crystallinity and molecular characteristics, which could be improved through blending with other biodegradable polymers such as poly(hydroxybutyrate) (PHB). Previous published studies have shown that the mechanical properties of such blends can be improved further. In this work, the effect of blending PHB with PLA on the photon- and neutron-shielding capabilities will be investigated using Geant4 over a wide energy range, as well as the effect of doping those blends with metal oxides. The results show that the shielding properties of the polymers are affected by blending with other polymers and by doping the polymer blends with different metal oxides, and they confirm that Geant4 is a very reliable tool that can simulate any material's shielding properties against photons and neutrons.

Keywords: biopolymer blends; PLA; PHB; photon; neutron; shielding; Geant4

check for updates

Citation: Akhdar, H.; Alshehri, M. Geant4 Simulation of Photon- and Neutron-Shielding Capabilities of Biopolymer Blends of Poly(lactic acid) and Poly(hydroxybutyrate). *Polymers* **2023**, *15*, 4257. https://doi.org/10.3390/polym15214257

Academic Editors: Juan J. Freire and Costas H. Vlahos

Received: 9 October 2023
Revised: 26 October 2023
Accepted: 27 October 2023
Published: 29 October 2023

Copyright: © 2023 by the authors. Licensee MDPI, Basel, Switzerland. This article is an open access article distributed under the terms and conditions of the Creative Commons Attribution (CC BY) license (https://creativecommons.org/licenses/by/4.0/).

1. Introduction

Biopolymers have been receiving more attention recently due to the environmental concerns in many applications. One of the most widely studied biopolymers is polylactic acid (PLA) because it is known for its availability, low cost, high transparency, thermal plasticity and good mechanical properties [1–4]. It is also biodegradable and biocompatible and can be produced from renewable resources, with properties that are very close to those of some synthetic fossil-fuel-based polymers. PLA plays an important role in many applications, ranging from the industrial to biomedical fields [5–7].

Despite the values of tensile strength and elastic modulus and the properties that make PLA very similar to high-performance polymers, it has some drawbacks, such as its brittleness and poor barrier properties, which restrict its range of application [8–12].

One of the strategies proposed to overcome those drawbacks is the formulation of PLA-based polymer blends. Recent studies have shown that a suitable polymer for PLA-based blend formation is poly (3-hydroxybutyrate) (PHB). PHB is a biodegradable thermoplastic that plays a role in many industrial applications [13–19]. PLA–PHB blends have been the focus of recent research because the combination of both biopolymers enhances their mechanical and tensile properties, making them more desirable in a wide range of applications [20–27]. Another strategy to enhance polymers' properties is to dope them with metal oxides. Many research works have studied the effect of different dopants on the optical and electrical properties of polymers. Recent research has avoided using lead oxides and focused instead on nontoxic metal oxides [28–30].

Radiation plays an important role in our lives, but it can cause damage either directly or indirectly by penetrating human bodies [31–34]. This is why researchers are constantly studying the radiation-shielding capabilities of materials used in industry and medicine, and polymers are receiving more attention in the radiation-shielding field because of their mechanical properties and their abilities to shield against radiation [3–40].

A recent study showed that doping Poly(lactic acid) (PLA)/Poly(ethylene glycol) (PEG) blended films with different amounts of lead increased their gamma-shielding abilities [41].

In this work, PLA–PHB blends were studied in terms of photon- and neutron-shielding capabilities. The shielding properties of pure PLA were compared to that of PLA-based blends with PHB at different percentages (10, 20 and 30%). The photon and neutron attenuation coefficients of the studied blends were theoretically investigated at a large energy range (from 10 to 2000 keV) using the Monte Carlo simulation toolkit Geant4.

Then, the PLA-based blends with PHB at different percentages (10–30%) were doped with 10% of different metal oxides, namely, zinc oxide (ZnO), iron oxide (Fe_2O_3), titanium oxide (Ti_2O) and magnesium oxide (MgO), and their effects on the photon- and neutron-shielding capabilities were also investigated using Geant4. The novelty of this work comes from studying the shielding abilities of the PLA/PHB blends and from doping the blends with metal oxides, which is presented theoretically using Geant4.

The Geant4 simulation reduced the time and cost needed to make such an investigation. It also enabled the study of different percentages at different energies and the effect of different dopants on the shielding capabilities of the studied polymer blends.

2. Materials

PLA and PHB are both biopolymers. The density of PLA is 1.24 g/cm^3, and the repeating unit is $(C_3H_4O_2)_n$, while the density of PHB is 1.19 g/cm^3 and the repeating unit is $(C_4H_6O_2)_n$, as shown in Figure 1. Table 1 summarizes the element weight fractions of both biopolymers [24]. The influence of blending the high-molecular-weight PHB with the low-molecular-weight PLA on the attenuation of the blends against radiation was studied.

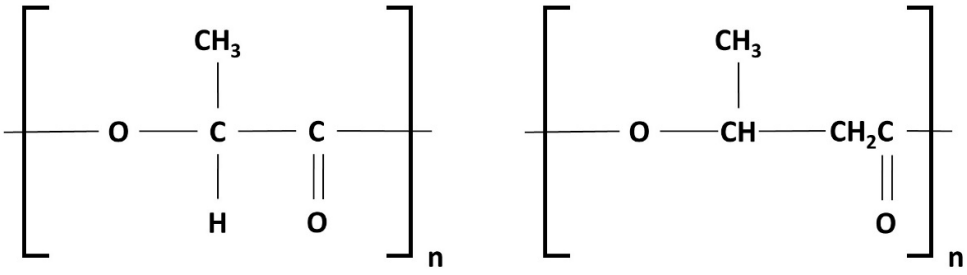


Figure 1. Repeating unit of PLA (**left**) and PHB (**right**) polymers.

Table 1. Element weight fractions in PLA and PHB.

Element	PLA	PHB
H (Hydrogen)	0.05595	0.07025
C (Carbon)	0.50001	0.55806
O (Oxygen)	0.44404	0.37169

3. Theory

3.1. Photon Attenuation

The photon mass attenuation coefficient of any material can be calculated using Equation (1) [42–45]:

$$I = I_0 e^{-\mu x} \quad (1)$$

When photons enter a material of thickness x with intensity I_0, it attenuates and its intensity is reduced to I [25]. Another important property when it comes to investigating any radiation-shielding material is the half-value layer which can be found using Equations (2) and (3):

$$HVL = \frac{\ln 2}{\mu} \tag{2}$$

$$\mu_m = \mu/\rho \tag{3}$$

where μ is the linear attenuation coefficient and ρ is the material density [37–40].

The total atomic cross-section can be calculated using Equation (4), where N_A is Avogadro's number and A_i is the atomic weight of an element of the compound, while the total electronic cross-section for the element is given by Equation (5) [42–45]:

$$\sigma_{t,a} = \frac{\mu_m}{N_A \sum_i^n (w_i/A_i)} \tag{4}$$

$$\sigma_{t,el} = \frac{1}{N_A} \sum_i^n \frac{f_i A_i}{Z_i} (\mu_{mt})_i \tag{5}$$

where f_i is the number of atoms of the element i relative to the total number of atoms of all elements in the compound and Z_i is the atomic number of the ith element in the compound. The effective atomic number (Z_{eff}) of the compound can be found from the ratio between the total atomic cross-section and the total electronic cross-section using Equation (6), and the effective electron density is given by Equation (7) [42–45]:

$$Z_{eff} = \frac{\sigma_{t,a}}{\sigma_{t,el}} \tag{6}$$

$$N_{eff} = \frac{\mu_m}{\sigma_{t,el}} \tag{7}$$

All these important parameters were investigated theoretically in this work on the PLA–PHB blends in the studied energy range.

3.2. Neutron Attenuation

The probability of neutron reactions with any material is expressed by the neutron-removing cross-section (Σ_R), which is given by Equation (8) [46–48]:

$$\Sigma_R = \sum_i \rho_i (\Sigma_R/\rho)_i \tag{8}$$

where ρ_i is the partial density and Σ_R/ρ is the mass removal cross-section, which can be calculated using Equation (9) for any compound where A is the atomic weight and Z is the atomic number [46–48].

$$\frac{\Sigma_R}{\rho} = 0.206 A^{-\frac{1}{3}} Z^{-0.294} \tag{9}$$

The fast neutron removal cross-section can be found for any element using Equations (10) and (11) [41–43]:

$$\Sigma_R = 0.190 Z^{-0.743} \quad \text{if } Z \leq 8 \tag{10}$$

$$\Sigma_R = 0.125 Z^{-0.565} \quad \text{if } Z > 8 \tag{11}$$

Equation (12) gives the mean free Path (λ), which is the distance that the neutron travels without interaction, and Equation (13) gives the HVL [46–48].

$$\lambda = \frac{1}{\Sigma_R} \tag{12}$$

$$HVL = \frac{\ln 2}{\Sigma_R} \quad (13)$$

These important neutron-shielding parameters were also investigated theoretically in the studied energy range for the PLA–PHB blends.

4. Methods

Geant4, a powerful Monte Carlo toolkit, version 11.02, is utilized in nuclear physics, nuclear engineering and medical physics [49]. Here, it was used to investigate the studied blends' photon- and neutron-shielding properties. A Geant4 code was developed to study the interactions of both gammas and neutrons in an energy range between 10 keV and 20 MeV. A source was placed in front of the investigated sample shooting monoenergetic gamma and neutron particles in the direction of the sample followed by a detector covered by a lead shield. The attenuation of both gammas and neutrons was measured by determining the ratio between the number of particles reaching the detector with and without the sample. For each energy, 1,000,000 monoenergetic particles were emitted in a direction perpendicular to the sample. Figure 2 shows a screenshot of the Geant4 simulation code used in this study. In order to validate the results obtained by the Geant4 code, the photon-shielding properties were compared to those found by EpiXS, which is a Windows-based program for photon attenuation, dosimetry and shielding based on the EPICS2017 and EPDL9 databases that can obtain the photon cross-section data for any sample [50]. Root, version 6.10/04, software was used to plot the figures presented in this article [51].

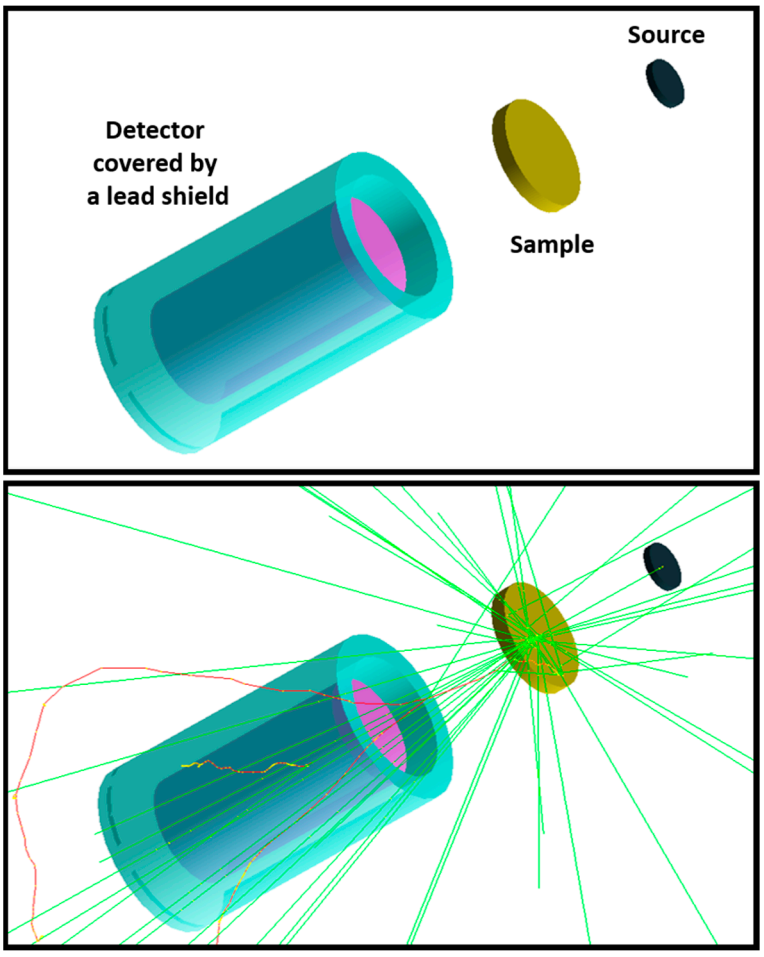


Figure 2. Visualization of the developed Geant4 code (green lines in the bottom image represent the photons or neutrons, and the red lines represent negatively charged particles).

5. PLA Photon-Shielding Properties and Validation of Geant4 Code Results

5.1. PLA Photon-Shielding Capbilities

The photon-shielding properties of PLA were investigated in a wide energy range from 10 keV to 20 MeV and compared to those found by EpiXS using Equation (14) in order to validate the results obtained by Geant4 (Table 2).

$$\Delta\% = \frac{(\text{Geant4 result} - \text{EpiXS result})}{\text{EpiXS result}} \times 100 \quad (14)$$

The results obtained from Geant4 show excellent agreement with those from EpiXS as the percentage differences between them were less than 1% in the case of the mass attenuation coefficients, with an average of 0.14% for the whole energy range. The percentage differences in the case of the estimates of HVLs were less than 1% as well, with an average of −0.14% for the whole energy range. In the case of the results of the effective atomic numbers and effective neutron densities, the results were in good agreement and had an average percentage difference of −1.57% and −1.61%, respectively; at lower energies, the differences between the results obtained from Geant4 and EpiXS were greater but did not exceed 10%. These results confirm that the Geant4 code is reliable in estimating the photon-shielding capabilities of any material.

Table 2. Photon-shielding properties of PLA.

Energy (keV)	Geant4	EpiXS	Δ%	Geant4	EpiXS	Δ%
	μ_m (cm²/g)			HVL (cm)		
10	3.8155	3.8541	−1.00%	0.1465	0.1450	1.01%
20	0.6288	0.6269	0.31%	0.8890	0.8917	−0.31%
30	0.3181	0.3162	0.59%	1.7575	1.7676	−0.57%
40	0.2387	0.2382	0.21%	2.3417	2.3468	−0.22%
50	0.2088	0.2071	0.80%	2.6777	2.6987	−0.78%
60	0.1919	0.1906	0.69%	2.9126	2.9330	−0.70%
70	0.1813	0.1799	0.80%	3.0830	3.1078	−0.80%
80	0.1728	0.1723	0.30%	3.2349	3.2445	−0.30%
90	0.1666	0.1660	0.37%	3.3555	3.3676	−0.36%
100	0.1610	0.1610	0.01%	3.4716	3.4723	−0.02%
200	0.1291	0.1299	−0.65%	4.3315	4.3018	0.69%
300	0.1123	0.1126	−0.28%	4.9786	4.9637	0.30%
400	0.1009	0.1008	0.15%	5.5393	5.5482	−0.16%
500	0.0924	0.0919	0.49%	6.0517	6.0795	−0.46%
600	0.0855	0.0850	0.55%	6.5344	6.5739	−0.60%
700	0.0799	0.0794	0.66%	6.9918	7.0422	−0.72%
800	0.0753	0.0747	0.86%	7.4254	7.4871	−0.82%
900	0.0713	0.0706	1.00%	7.8454	7.9183	−0.92%
1000	0.0676	0.0671	0.75%	8.2726	8.3311	−0.70%
2000	0.0469	0.0468	0.13%	11.9291	11.9343	−0.04%
3000	0.0375	0.0376	−0.24%	14.9209	14.8707	0.34%
4000	0.0320	0.0322	−0.56%	17.4414	17.3711	0.40%
5000	0.0285	0.0286	−0.45%	19.6034	19.5246	0.40%
6000	0.0260	0.0261	−0.50%	21.4727	21.3925	0.37%
7000	0.0242	0.0243	−0.29%	23.1003	23.0326	0.29%
8000	0.0228	0.0229	−0.27%	24.5232	24.4511	0.29%
9000	0.0217	0.0217	−0.20%	25.7737	25.7091	0.25%
10,000	0.0208	0.0208	−0.19%	26.8773	26.8239	0.20%
20,000	0.0169	0.0169	0.00%	33.0325	33.0776	−0.14%

Table 2. *Cont.*

Energy (keV)	Geant4	EpiXS	Δ%	Geant4	EpiXS	Δ%
	Z_{eff}			N_{eff} ($\times 10^{23}$)		
10	6.107	6.121	−0.22%	4.700	4.603	2.10%
20	5.486	5.880	−6.71%	4.190	4.423	−5.26%
30	4.897	5.392	−9.19%	3.710	4.056	−8.52%
40	4.583	4.938	−7.19%	3.460	3.714	−6.83%
50	4.470	4.673	−4.34%	3.360	3.515	−4.40%
60	4.395	4.523	−2.83%	3.300	3.402	−3.00%
70	4.360	4.437	−1.74%	3.270	3.337	−2.02%
80	4.314	4.384	−1.59%	3.240	3.297	−1.73%
90	4.302	4.349	−1.09%	3.230	3.271	−1.26%
100	4.277	4.326	−1.13%	3.210	3.254	−1.34%
200	4.219	4.261	−0.99%	3.160	3.205	−1.41%
300	4.231	4.251	−0.48%	3.170	3.198	−0.86%
400	4.248	4.247	0.01%	3.180	3.195	−0.46%
500	4.260	4.246	0.33%	3.190	3.194	−0.11%
600	4.266	4.245	0.49%	3.200	3.193	0.22%
700	4.271	4.245	0.62%	3.200	3.193	0.23%
800	4.275	4.245	0.72%	3.200	3.192	0.24%
900	4.279	4.244	0.82%	3.210	3.192	0.56%
1000	4.270	4.244	0.61%	3.200	3.192	0.25%
2000	4.249	4.255	−0.13%	3.190	3.200	−0.31%
3000	4.252	4.282	−0.71%	3.190	3.221	−0.96%
4000	4.273	4.316	−1.01%	3.200	3.246	−1.43%
5000	4.299	4.352	−1.22%	3.230	3.273	−1.32%
6000	4.327	4.388	−1.38%	3.250	3.300	−1.52%
7000	4.358	4.422	−1.45%	3.270	3.326	−1.68%
8000	4.385	4.454	−1.55%	3.290	3.350	−1.79%
9000	4.413	4.485	−1.60%	3.320	3.373	−1.57%
10,000	4.441	4.513	−1.59%	3.340	3.394	−1.60%
20,000	4.662	4.705	−0.91%	3.510	3.538	−0.80%

5.2. PLA Neutron-Shielding Capabilities

In order to verify the Geant4 results in the case of the neutron-shielding properties of simulated materials, the fast neutron removal cross-section of PLA was estimated using Equations (9)–(11), as shown in Table 3.

Table 3. Fast neutron removal cross-section of PLA.

Element	Weight Fraction	Σ_R/ρ (cm^2/g)	Partial Density (g/cm^3)	Σ_R (cm^{-1})
H (Hydrogen)	0.0559	0.19000	0.0694	0.013181
C (Carbon)	0.5000	0.05019	0.6200	0.031118
O (Oxygen)	0.4440	0.04053	0.5506	0.022316
Total fast neutron removal cross-section = 0.066616				

The fast neutron removal cross-section of PLA was simulated using Geant4 and was equal to 0.060894 cm^{-1} which is in very good agreement with the neutron removal cross-section found in Table 3, indicating that Geant4 can reliably predict the neutron-shielding abilities of any material. The neutron removal cross-sections and half-value layers of PLA were investigated using Geant4 in an energy range from 10 keV to 20,000 keV, as shown in Table 4.

As the results obtained by Geant4 were validated and the photon- and neutron-shielding properties of PLA were verified, we can estimate the effect of blending PLA with PHB on the shielding properties and the effect of doping those blends with different metal oxides.

Table 4. Neutron-shielding properties of PLA.

Energy (keV)	Σ_R (cm^2/g)	*HVL* (cm)
10	0.8310	0.6726
20	0.7956	0.7026
30	0.7603	0.7353
40	0.7248	0.7713
50	0.7043	0.7937
60	0.6837	0.8177
70	0.6631	0.8430
80	0.6424	0.8702
90	0.6216	0.8993
100	0.6008	0.9305
200	0.4864	1.1492
300	0.4222	1.3239
400	0.4345	1.2865
500	0.3714	1.5053
600	0.3199	1.7476
700	0.2989	1.8702
800	0.2803	1.9946
900	0.2742	2.0390
1000	0.3456	1.6176
2000	0.1660	3.3680
3000	0.1269	4.4060
4000	0.1478	3.7826
5000	0.1023	5.4648
6000	0.1038	5.3863
7000	0.0766	7.2967
8000	0.0997	5.6095
9000	0.0832	6.7205
10,000	0.0830	6.7310
20,000	0.0816	6.8480

6. Effect of PLA Blending with PHB on the PLA-Shielding Properties

6.1. PLA–PHB Blends' Photon-Shielding Capabilities

The photon-shielding properties of all the investigated blends were compared using Geant4 in the same energy range (Table 5). The linear attenuation coefficients of all the studied blends were plotted against that of PLA to more easily visualize the comparison (Figure 3).

Table 5. Photon-shielding properties of PLA–PHB blends.

Energy (keV)	μ_m (cm^2/g)		
	90% PLA–10% PHB	**80% PLA–20% PHB**	**70% PLA–30% PHB**
10	3.7870	3.7584	3.7298
20	0.6255	0.6222	0.6190
30	0.3173	0.3165	0.3157
40	0.2385	0.2383	0.2382
50	0.2088	0.2088	0.2088
60	0.1920	0.1921	0.1922
70	0.1815	0.1816	0.1817
80	0.1730	0.1731	0.1733
90	0.1668	0.1669	0.1671
100	0.1612	0.1614	0.1616
200	0.1292	0.1294	0.1295

Table 5. *Cont.*

Energy (keV)	μ_m (cm^2/g)		
	90% PLA–10% PHB	**80% PLA–20% PHB**	**70% PLA–30% PHB**
300	0.1124	0.1126	0.1127
400	0.1010	0.1012	0.1013
500	0.0925	0.0926	0.0927
600	0.0857	0.0858	0.0859
700	0.0801	0.0802	0.0803
800	0.0754	0.0755	0.0756
900	0.0713	0.0714	0.0715
1000	0.0677	0.0678	0.0678
2000	0.0469	0.0470	0.0470
3000	0.0375	0.0376	0.0376
4000	0.0321	0.0321	0.0322
5000	0.0285	0.0286	0.0286
6000	0.0261	0.0261	0.0261
7000	0.0242	0.0242	0.0243
8000	0.0228	0.0228	0.0228
9000	0.0217	0.0217	0.0217
10,000	0.0208	0.0208	0.0208
20,000	0.0169	0.0169	0.0169
Energy (keV)	Z_{eff}		
	90% PLA–10% PHB	**80% PLA–20% PHB**	**70% PLA–30% PHB**
10	1.466	1.455	1.444
20	1.311	1.304	1.297
30	1.163	1.161	1.158
40	1.085	1.084	1.084
50	1.057	1.057	1.057
60	1.038	1.038	1.039
70	1.029	1.030	1.031
80	1.018	1.019	1.020
90	1.015	1.016	1.017
100	1.009	1.010	1.010
200	0.995	0.996	0.997
300	0.998	0.999	1.000
400	1.002	1.003	1.004
500	1.005	1.006	1.007
600	1.006	1.007	1.009
700	1.007	1.008	1.010
800	1.008	1.009	1.011
900	1.009	1.010	1.012
1000	1.007	1.008	1.010
2000	1.002	1.003	1.005
3000	1.003	1.004	1.005
4000	1.008	1.009	1.010
5000	1.014	1.015	1.016
6000	1.021	1.022	1.023
7000	1.029	1.030	1.030
8000	1.035	1.036	1.037
9000	1.042	1.043	1.043
10,000	1.049	1.050	1.050
20,000	1.103	1.103	1.102

Table 5. *Cont.*

Energy (keV)	N_{eff} ($\times 10^{23}$)		
	90% PLA–10% PHB	80% PLA–20% PHB	70% PLA–30% PHB
10	4.67	4.63	4.60
20	4.17	4.15	4.13
30	3.70	3.69	3.69
40	3.45	3.45	3.45
50	3.36	3.36	3.36
60	3.30	3.31	3.31
70	3.28	3.28	3.28
80	3.24	3.24	3.25
90	3.23	3.23	3.24
100	3.21	3.22	3.22
200	3.17	3.17	3.17
300	3.18	3.18	3.18
400	3.19	3.19	3.20
500	3.20	3.20	3.21
600	3.20	3.21	3.21
700	3.21	3.21	3.21
800	3.21	3.21	3.22
900	3.21	3.22	3.22
1000	3.20	3.21	3.21
2000	3.19	3.19	3.20
3000	3.19	3.20	3.20
4000	3.21	3.21	3.22
5000	3.23	3.23	3.24
6000	3.25	3.25	3.26
7000	3.27	3.28	3.28
8000	3.30	3.30	3.30
9000	3.32	3.32	3.32
10,000	3.34	3.34	3.34
20,000	3.51	3.51	3.51

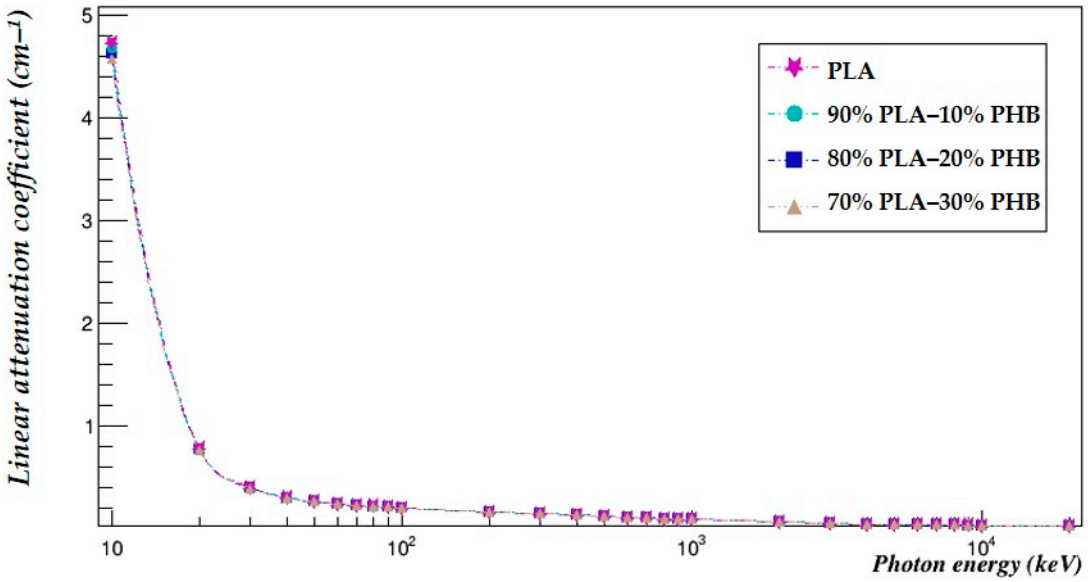


Figure 3. The linear attenuation coefficients of the investigated blends.

6.2. PLA–PHB Blends' Neutron-Shielding Capabilities

The neutron-shielding properties of the investigated blends were compared using Geant4 in the same energy range (Table 6). The linear removal cross-sections of all the

studied blends were plotted against that of PLA to more easily visualize the comparison (Figure 4).

Table 6. Neutron-shielding properties of PLA–PHB blends.

Energy (keV)	Σ_R (cm^2/g)		
	90% PLA–10% PHB	**80% PLA–20% PHB**	**70% PLA–30% PHB**
10	0.8480	0.8646	0.8816
20	0.8117	0.8275	0.8436
30	0.7753	0.7904	0.8055
40	0.7391	0.7533	0.7674
50	0.7180	0.7317	0.7454
60	0.6968	0.7101	0.7233
70	0.6758	0.6885	0.7012
80	0.6546	0.6668	0.6790
90	0.6332	0.6449	0.6566
100	0.6120	0.6231	0.6343
200	0.4949	0.5034	0.5119
300	0.4292	0.4362	0.4431
400	0.4397	0.4447	0.4498
500	0.3764	0.3815	0.3866
600	0.3247	0.3296	0.3344
700	0.3035	0.3080	0.3126
800	0.2845	0.2887	0.2929
900	0.2779	0.2816	0.2854
1000	0.3478	0.3500	0.3522
2000	0.1685	0.1711	0.1736
3000	0.1288	0.1308	0.1328
4000	0.1495	0.1511	0.1528
5000	0.1038	0.1052	0.1067
6000	0.1049	0.1060	0.1071
7000	0.0777	0.0787	0.0798
8000	0.1009	0.1022	0.1035
9000	0.0841	0.0849	0.0858
10,000	0.0838	0.0846	0.0854
20,000	0.0820	0.0823	0.0828
Energy (keV)	***HVL* (cm)**		
	90% PLA–10% PHB	**80% PLA–20% PHB**	**70% PLA–30% PHB**
10	0.6619	0.6518	0.6419
20	0.6915	0.6810	0.6707
30	0.7239	0.7129	0.7025
40	0.7594	0.7481	0.7373
50	0.7817	0.7702	0.7591
60	0.8054	0.7936	0.7823
70	0.8305	0.8185	0.8070
80	0.8574	0.8452	0.8334
90	0.8863	0.8738	0.8618
100	0.9171	0.9043	0.8921
200	1.1341	1.1194	1.1054
300	1.3077	1.2920	1.2769
400	1.2766	1.2671	1.2580
500	1.4910	1.4772	1.4638
600	1.7284	1.7099	1.6919
700	1.8496	1.8297	1.8103
800	1.9730	1.9520	1.9316
900	2.0198	2.0010	1.9829
1000	1.6138	1.6101	1.6064
2000	3.3305	3.2944	3.2594
3000	4.3562	4.3084	4.2621
4000	3.7555	3.7293	3.7038
5000	5.4091	5.3548	5.3020
6000	5.3519	5.3174	5.2852
7000	7.2265	7.1584	7.0925
8000	5.5603	5.5124	5.4659
9000	6.6774	6.6354	6.5947
10,000	6.6943	6.6585	6.6235
20,000	6.8481	6.8511	6.8307

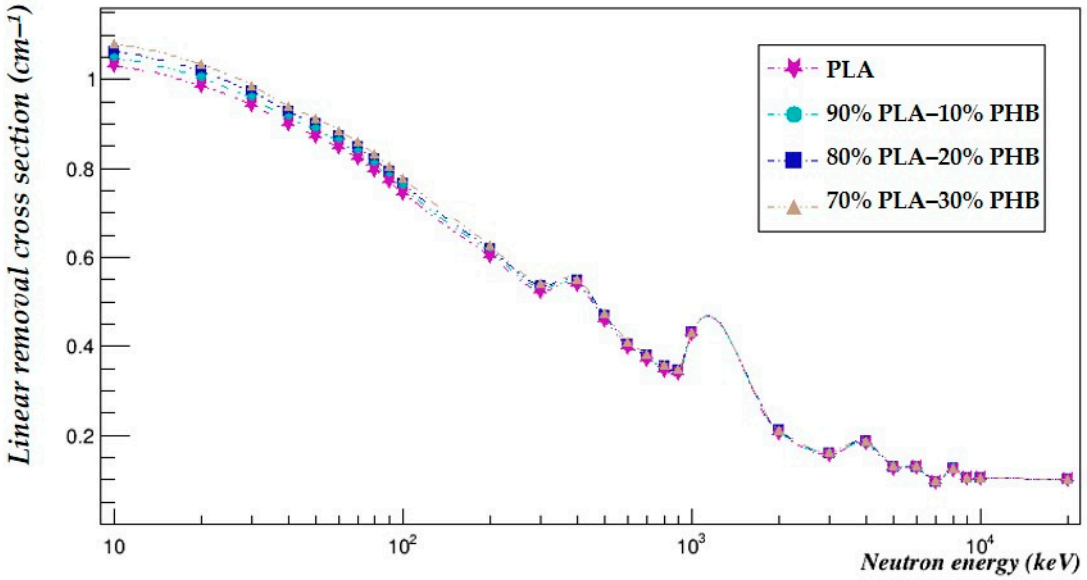


Figure 4. The linear removal cross-sections of the investigated blends.

7. Effect of Metal Oxide Doping on PLA–PHB Blends' Shielding Properties

The photon- and neutron-shielding properties of the 90–10% and the 70–30% blends doped with 10% of selected metal oxides (ZnO, Fe_2O_3, TiO_2 and MgO) were compared using Geant4 in the same energy range (Figures 5–8).

7.1. Effect of Metal Oxide Doping on the PLA–PHB Blends' Photon-Shielding Capabilities

Figures 5 and 6 represent the photon-shielding properties of the 90–10% and the 70–30% blends doped with 10% of selected metal oxides (ZnO, Fe_2O_3, TiO_2 and MgO).

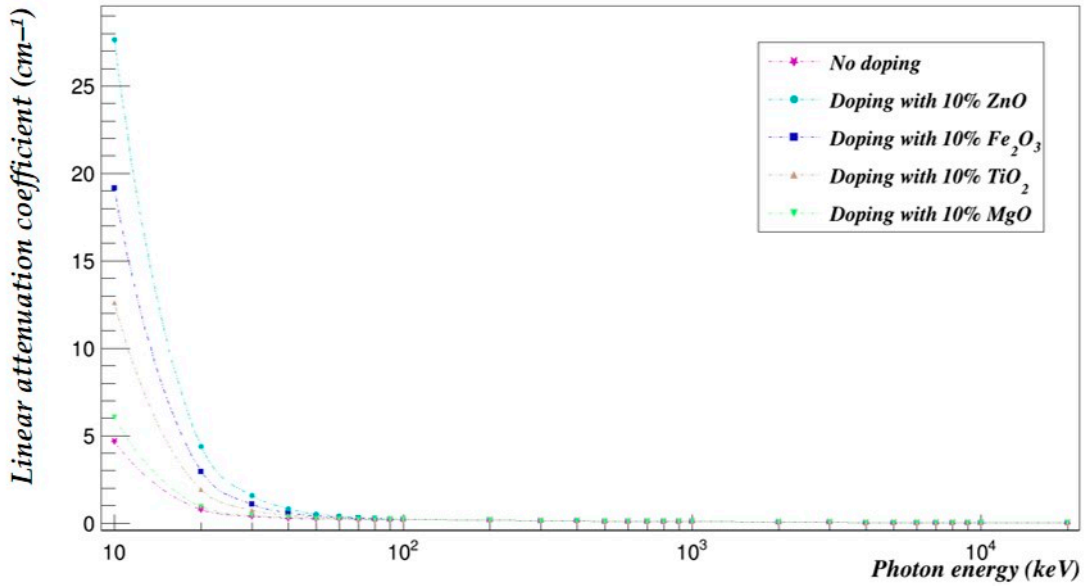


Figure 5. The photon linear attenuation coefficients of the PLA–PHB (90–10%) blend doped with 10% metal oxide.

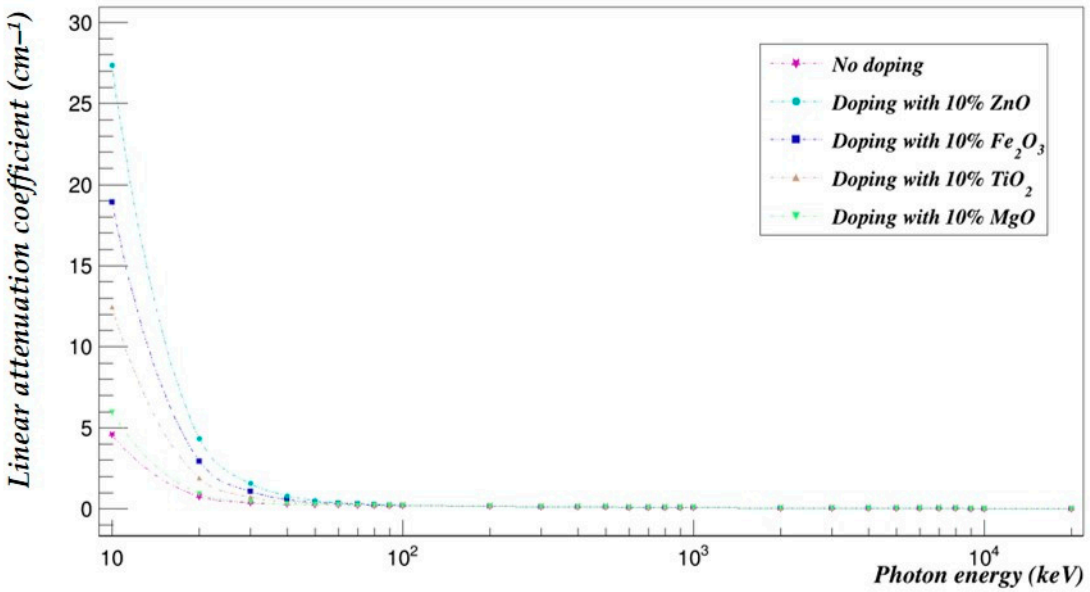


Figure 6. The photon linear attenuation coefficients of the PLA–PHB (70–30%) blend doped with 10% metal oxide.

7.2. Effect of Metal Oxide Doping on the PLA–PHB Blends' Neutron-Shielding Capabilities

Figures 7 and 8 represent the neutron-shielding properties of the 90–10% and the 70–30% blends doped with 10% of selected metal oxides (ZnO, Fe_2O_3, TiO_2 and MgO).

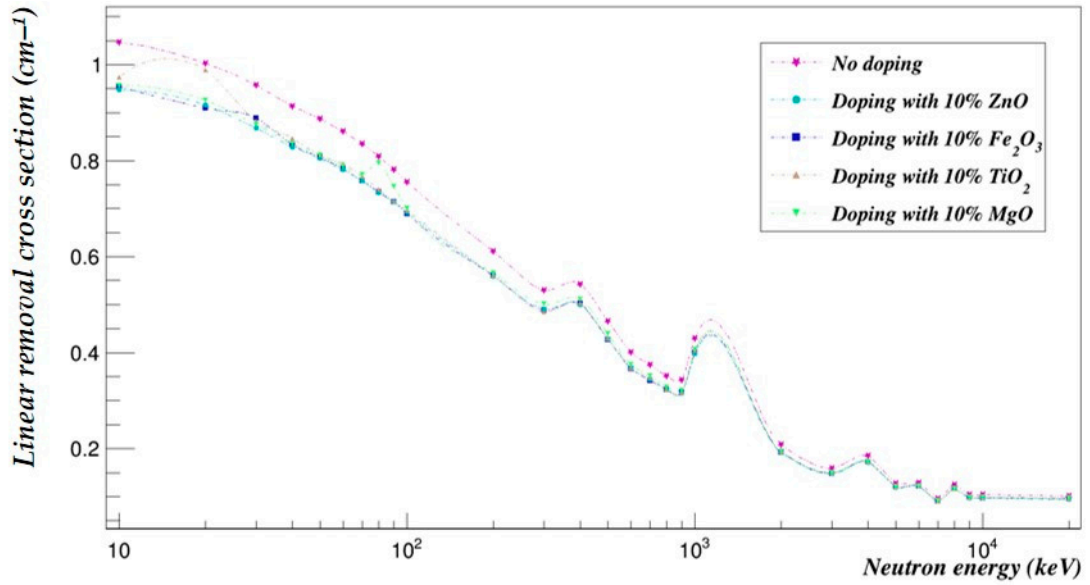


Figure 7. The neutron linear removal cross-sections of the PLA–PHB (90–10%) blend doped with 10% metal oxide.

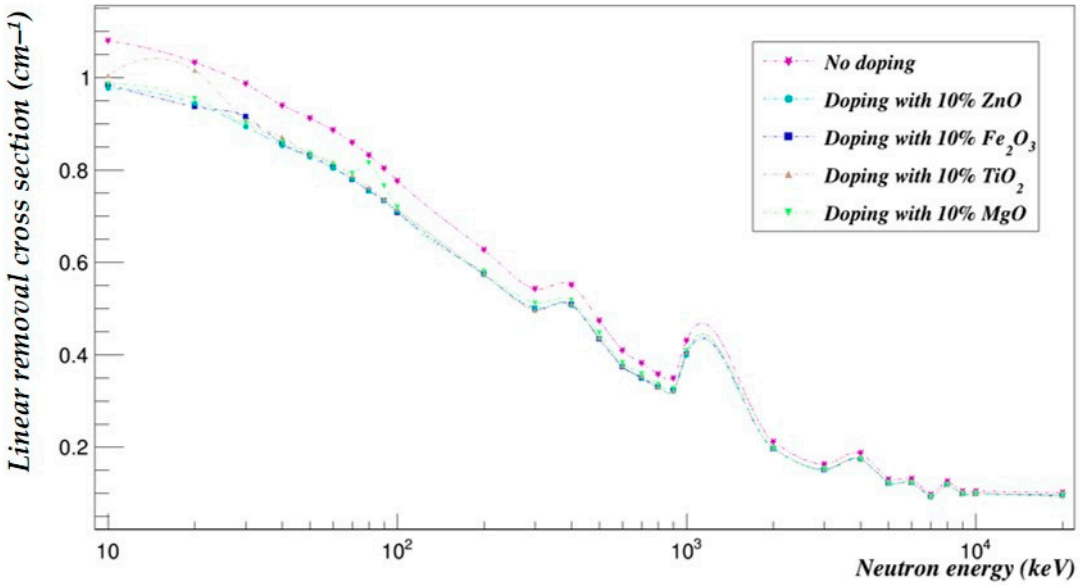


Figure 8. The neutron linear removal cross-sections of the PLA–PHB (70–30%) blend doped with 10% metal oxide.

8. Discussion

The results show that the mass attenuations of the 90–10% PLA–PHB blend decreased compared to those of PLA in an energy range of 10 to 40 keV by 0.08% to 0.75% and at an energy of 20,000 keV by 0.04%. In addition, the mass attenuations of the blend with 80–20% fractions decreased from 0.15% to 1.5% at energies ranging from 10 keV to 40 keV and by 0.07% at 20,000 keV. On the other hand, the mass attenuations of the blend with 70–30% fractions decreased from 0.23% to 2.25% at energies ranging from 10 keV to 40 keV and by 0.11% at 20,000 keV. Meanwhile, at all the other studied energies, the mass attenuation coefficients increased by an average of 0.1% for the 90–10% blend, 0.2% for the 80–20% blend and 0.3% for the 70–30% blend.

The linear attenuation coefficients of the 90–10%, 80–20% and 70–30% blends decreased by an average of 0.38%, 0.75% and 1.13%, while the HVL increased by an average of 0.38%, 0.76% and 1.15%, respectively.

The blending decreased the ability of PLA to shield against photons especially at low energies and very-high-energy photons. In addition, the higher the fraction of PHB added to the blend, the lower the photon-shielding capability of the blend.

The results show that the neutron removal cross-sections were increased by an average of 1.51% for the 90–10% blend, 3.01% for the 80–20% blend and 4.53% for the 70–30% blend.

The neutron half-value layers were decreased by an average of 1.09% for the 90–10% blend, 2.13% for the 80–20% blend and 3.15% for the 70–30% blend.

The blending increased the capability of PLA to attenuate neutrons in the whole studied energy range, and the ability of the blends to shield against neutrons increased with the fraction of PHB added to the blend.

The results clearly show that the neutron-shielding capabilities are affected by the blending of the biopolymers more than the photon-shielding capabilities. These results also show the influence of the molecular weight of polymers on photon- and neutron-shielding abilities.

The photon-shielding abilities of the 90–10% and 70–30% blends were increased in the studied energy range especially at low photon energies. ZnO had the most impact on the attenuation coefficients of the 90–10% blend with an average increase of 59.91%, followed by Fe_2O_3, which increased the photon-shielding abilities by an average of 35.79% over the investigated energy range; then TiO_2, which increased the attenuation coefficients by an average of 18.49%; and finally, MgO, which increased them by an average of 2.64%. On the other hand, the 70–30% blend's photon attenuation coefficients were increased by an

average of 60.39% when it was doped with 10% ZnO, 36.08% with Fe_2O_3, 18.64% with TiO_2 and 2.67% with MgO.

The neutron-shielding capabilities of both the 90–10% and 70–30% blends were decreased by an average of 14.10% and 7.90% when doped with ZnO, 13.94% and 7.73% with Fe_2O_3, 13.23% and 6.98% with TiO_2 and 12.65% and 6.38% with MgO, respectively.

9. Conclusions

The blending of polymers could enhance many properties that could be used in many applications. One of the properties affected by polymer blending is the radiation-shielding capabilities. In this work, the photon- and neutron-shielding abilities of PLA–PHB blends were simulated using the Monte Carlo toolkit Geant4.

The results show the following:

- The photon-shielding properties decreased when blending PHB with PLA, while the neutron-shielding abilities were improved by blending.
- Doping the PLA–PHB blends with metal oxides enhanced the photon-shielding capabilities of the studied blends and slightly reduced their neutron-shielding capabilities.
- Geant4 is a very reliable tool which can be used to simulate the interactions of any radiation type with any material and, hence, evaluate the shielding capabilities of different materials.

The use and application of the blends should be considered when choosing the right type and fraction of polymers to blend. On the other hand, doping with metal oxides could affect the shielding properties of different polymer blends and the type of dopants must be considered based on the desired applications because they could affect the photon- and neutron-shielding abilities in different ways.

Author Contributions: Conceptualization, H.A; methodology, H.A.; software, H.A and M.A.; validation, H.A.; formal analysis, H.A.; investigation, H.A. and M.A.; resources, H.A. and M.A.; data curation, H.A.; writing—original draft preparation, H.A. and M.A.; writing—review and editing, H.A. and M.A.; visualization, H.A.; supervision, H.A.; funding acquisition, H.A. and M.A. All authors have read and agreed to the published version of the manuscript.

Funding: This research received no external funding.

Institutional Review Board Statement: Not applicable.

Data Availability Statement: The data presented in this study are available on request from the corresponding author.

Conflicts of Interest: The authors declare no conflict of interest.

References

1. Laycock, B.; Halley, P.; Pratt, S.; Werker, A.; Lant, P. The chemomechanical properties of microbial polyhydroxyalkanoates. *Prog. Polym. Sci.* **2014**, *39*, 397–442. [CrossRef]
2. Tarrahi, R.; Fathi, Z.; Seydibeyoğlu, M.Ö.; Doustkhah, E.; Khataee, A. Polyhydroxyalkanoates (PHA): From production to nanoarchitecture. *Int. J. Biol. Macromol.* **2020**, *146*, 596–619. [CrossRef]
3. Dintcheva, N.T.; Arrigo, R.; Baiamonte, M.; Rizzarelli, P.; Curcuruto, G. Concentration-dependent anti-/pro-oxidant activity of natural phenolic compounds in bio-polyesters. *Polym. Degrad. Stab.* **2017**, *142*, 21–28. [CrossRef]
4. Stloukal, P.; Kalendova, A.; Mattausch, H.; Laske, S.; Holzer, C.; Koutny, M. The influence of a hydrolysis-inhibiting additive on the degradation and biodegradation of PLA and its nanocomposites. *Polym. Test.* **2015**, *41*, 124–132. [CrossRef]
5. Mokhena, T.C.; Sefadi, J.S.; Sadiku, E.R.; John, M.J.; Mochane, M.J.; Mtibe, A. Thermoplastic Processing of PLA/Cellulose Nanomaterials Composites. *Polymers* **2018**, *10*, 1363. [CrossRef] [PubMed]
6. Gonçalves, C.; Gonçalves, I.C.; Magalhães, F.D.; Pinto, A.M. Poly (lactic acid) Composites Containing Carbon-Based Nanomaterials: A Review. *Polymers* **2017**, *9*, 269. [CrossRef] [PubMed]
7. Burzic, I.; Pretschuh, C.; Kaineder, D.; Eder, G.; Smilek, J.; Másilko, J.; Kateryna, W. Impact modification of PLA using biobased biodegradable PHA biopolymers. *Eur. Polym. J.* **2019**, *114*, 32–38. [CrossRef]
8. Requena, R.; Jiménez, A.; Vargas, M.; Chiralt, A. Effect of plasticizers on thermal and physical properties of compression-moulded poly[(3-hydroxybutyrate)-co-(3-hydroxyvalerate)] films. *Polym. Test.* **2016**, *56*, 45–53. [CrossRef]

9. Hamad, K.; Kaseem, M.; Yang, H.W.; Deri, F.; Ko, Y.G. Properties and medical applications of polylactic acid: A review. *Express Polym. Lett.* **2015**, *9*, 435–455. [CrossRef]
10. Battegazzore, D.; Abt, T.; Maspoch, M.L.; Frache, A. Multilayer cotton fabric bio-composites based on PLA and PHB copolymer for industrial load carrying applications. *Compos. Part B Eng.* **2019**, *163*, 761–768. [CrossRef]
11. Liu, H.; Zhang, J. Research progress in toughening modification of poly(lactic acid). *J. Polym. Sci. Part B Polym. Phys.* **2011**, *49*, 1051–1083. [CrossRef]
12. Jin, F.-L.; Hu, R.-R.; Park, S.-J. Improvement of thermal behaviors of biodegradable poly (lactic acid) polymer: A review. *Compos. Part B Eng.* **2018**, *164*, 287–296. [CrossRef]
13. Lenz, A.R.W.; Marchessault, R.H. Bacterial Polyesters: Biosynthesis, Biodegradable Plastics and Biotechnology. *Biomacromolecules* **2005**, *6*, 1–8. [CrossRef] [PubMed]
14. Peña, C.; Castillo, T.; García, A.; Millán, M.; Segura, D. Biotechnological strategies to improve production of microbial poly-(3-hydroxybutyrate): A review of recent research work. *Microb. Biotechnol.* **2014**, *7*, 278–293. [CrossRef]
15. Chen, G.-Q.; Wu, Q. The application of polyhydroxyalkanoates as tissue engineering materials. *Biomaterials* **2005**, *26*, 6565–6578. [CrossRef] [PubMed]
16. Snell, K.D.; Peoples, O.P. PHA bioplastic: A value-added coproduct for biomass biorefineries. *Biofuels Bioprod. Biorefining Innov. A Sustain. Econ.* **2009**, *3*, 456–467. [CrossRef]
17. Baltieri, R.C.; Innocentini Mei, L.H.; Bartoli, J. Study of the influence of plasticizers on the thermal and mechanical properties of poly(3-hydroxybutyrate) compounds. *Macromol. Symp.* **2003**, *197*, 33–44. [CrossRef]
18. Volova, T.G. *Polyhydroxyalkanoates-Plastic Materials of the 21st Century: Production, Properties, Applications*; Nova Science Publishers: Hauppauge, NY, USA, 2004.
19. Wady, P.; Wasilewski, A.; Brock, L.; Edge, R.; Baidak, A.; McBride, C.; Leay, L.; Griffiths, A.; Vallés, C. Effect of ionising radiation on the mechanical and structural properties of 3D printed plastics. *Addit. Manuf.* **2019**, *31*, 100907. [CrossRef]
20. Abdelwahab, M.A.; Flynn, A.; Chiou, B.-S.; Imam, S.; Orts, W.; Chiellini, E. Thermal, mechanical and morphological characterization of plasticized PLA–PHB blends. *Polym. Degrad. Stab.* **2012**, *97*, 1822–1828. [CrossRef]
21. Arrieta, M.P.; Samper, M.D.; Aldas, M.; López, J. On the Use of PLA-PHB Blends for Sustainable Food Packaging Applications. *Materials* **2017**, *10*, 1008. [CrossRef]
22. Dobrovszky, K.; Ronkay, F. Influence of morphology and compatibilizer on burning behavior of PET/HDPE blend. In Proceedings of the Regional Conference Graz 2015–Polymer Processing Society PPS, Graz, Austria, 21–25 September 2015; p. 080012.
23. D'anna, A.; Arrigo, R.; Frache, A. Rheology, Morphology and Thermal Properties of a PLA/PHB/Clay Blend Nanocomposite: The Influence of Process Parameters. *J. Polym. Environ.* **2021**, *30*, 102–113. [CrossRef]
24. D'anna, A.; Arrigo, R.; Frache, A. PLA/PHB Blends: Biocompatibilizer Effects. *Polymers* **2019**, *11*, 1416. [CrossRef] [PubMed]
25. Lacoste, C.; Gallard, B.; Lopez-Cuesta, J.-M.; Kalaoglu-Altan, O.I.; De Clerck, K. Development of Bionanocomposites Based on Poly(3-Hydroxybutyrate-co-3-Hydroxyvalerate)/PolylActide Blends Reinforced with Cloisite 30B. *J. Funct. Biomater.* **2020**, *11*, 64. [CrossRef]
26. Patel, M.K.; Zaccone, M.; De Brauwer, L.; Nair, R.; Monti, M.; Martinez-Nogues, V.; Frache, A.; Oksman, K. Improvement of Poly(lactic acid)-Poly(hydroxy butyrate) Blend Properties for Use in Food Packaging: Processing, Structure Relationships. *Polymers* **2022**, *14*, 5104. [CrossRef] [PubMed]
27. Puglia, D.; Fortunati, E.; D'amico, D.A.; Miri, V.; Stoclet, G.; Manfredi, L.B.; Cyras, V.P.; Kenny, J.M. Influence of Processing Conditions on Morphological, Thermal and Degradative Behavior of Nanocomposites Based on Plasticized Poly(3-hydroxybutyrate) and Organo-Modified Clay. *J. Polym. Environ.* **2015**, *24*, 12–22. [CrossRef]
28. Bekhoukh, A.; Moulefera, I.; Sabantina, L.; Benyoucef, A. Development, Investigation, and Comparative Study of the Effects of Various Metal Oxides on Optical Electrochemical Properties Using a Doped PANI Matrix. *Polymers* **2021**, *13*, 3344. [CrossRef]
29. Obreja, P.; Cristea, D.; Purica, M.; Gavrila, R.; Comanescu, F. Polymers doped with metal oxide nanoparticles with controlled refractive index. *Polimery* **2007**, *52*, 679–685. [CrossRef]
30. Abbas, Y.M.; Hasan, A.A. Optical Properties Study of Polypyrrole doped with TiO_2, WO_3, Fe_2O_3 and SnO_2 Nanoparticles. *IOP Conf. Ser. Mater. Sci. Eng.* **2020**, *928*, 072017. [CrossRef]
31. Yin, S.; Wang, H.; Wang, S.; Zhang, J.; Zhu, Y. Effect of B_2O_3 on the Radiation Shielding Performance of Telluride Lead Glass System. *Crystals* **2022**, *12*, 178. [CrossRef]
32. Rammah, Y.; El-Agawany, F.; Abu El Soad, A.; Yousef, E.; El-Mesady, I. Ionizing radiation attenuation competences of gallium germanate-tellurite glasses utilizing MCNP5 simulation code and Phy-X/PSD program. *Ceram. Int.* **2020**, *46*, 22766–22773. [CrossRef]
33. Hamad, R.; Mhareb, M.; Alajerami, Y.; Sayyed, M.; Saleh, G.; Hamad, M.K.; Ziq, K. A comprehensive ionizing radiation shielding study of FexSe0.5Te0.5 alloys with various iron concentrations. *J. Alloy. Compd.* **2020**, *858*, 157636. [CrossRef]
34. Olarinoye, I.O.; Alomairy, S.; Sriwunkum, C.; Al-Buriahi, M.S. Effect of Ag_2O/V_2O_5 substitution on the radiation shielding ability of tellurite glass system via XCOM approach and FLUKA simulations. *Phys. Scr.* **2021**, *96*, 065308. [CrossRef]
35. Akhdar, H. Theoretical Investigation of Gamma- and Neutron-Shielding Properties of Polysulfone (PSU) Polymer Material Using Geant4. *Polymers* **2022**, *14*, 3374. [CrossRef]
36. Akhdar, H.; Alotaibi, R. Geant4 Simulation of the Effect of Different Composites on Polyimide Photon and Neutron Shielding Properties. *Polymers* **2023**, *15*, 1973. [CrossRef]

37. Akhdar, H.; Marashdeh, M.; AlAqeel, M. Investigation of gamma radiation shielding properties of polyethylene glycol in the energy range from 8.67 to 23.19 keV. *Nucl. Eng. Technol.* **2021**, *54*, 701–708. [CrossRef]
38. Al-Buriahi, M.S.; Eke, C.; Alomairy, S.; Yildirim, A.; Alsaeedy, H.I.; Sriwunkum, C. Radiation attenuation properties of some commercial polymers for advanced shielding applications at low energies. *Polym. Adv. Technol.* **2021**, *32*, 2386–2396. [CrossRef]
39. Sayyed, M. Investigation of shielding parameters for smart polymers. *Chin. J. Phys.* **2016**, *54*, 408–415. [CrossRef]
40. Abdali, K. Crystal Structural, Morphological and Gamma Ray Shielding (γ-S) Efficiency of PVA/PAAM/PAA Polymer Blend Loaded with Silver Nanoparticles via Casting Method. *Research Square*, 11 November 2021. [CrossRef]
41. Yilmaz, M.; Pekdemir, M.E.; Öner, E. Evaluation of Pb doped Poly(lactic acid) (PLA)/Poly(ethylene glycol) (PEG) blend composites regarding physicochemical and radiation shielding properties. *Radiat. Phys. Chem.* **2023**, *202*, 110509. [CrossRef]
42. Hubbell, J. Photon mass attenuation and energy-absorption coefficients. *Int. J. Appl. Radiat. Isot.* **1982**, *33*, 1269–1290. [CrossRef]
43. Kaewkhao, J.; Laopaiboon, J.; Chewpraditkul, W. Determination of effective atomic numbers and effective electron densities for Cu/Zn alloy. *J. Quant. Spectrosc. Radiat. Transf.* **2008**, *109*, 1260–1265. [CrossRef]
44. Un, A.; Demir, F. Determination of mass attenuation coefficients, effective atomic numbers and effective electron numbers for heavy-weight and normal-weight concretes. *Appl. Radiat. Isot.* **2013**, *80*, 73–77. [CrossRef] [PubMed]
45. Singh, K.; Singh, H.; Sharma, V.; Nathuram, R.; Khanna, A.; Kumar, R.; Bhatti, S.S.; Sahota, H.S. Gamma-ray attenuation coefficients in bismuth borate glasses. *Nucl. Instruments Methods Phys. Res. Sect. B Beam Interactions Mater. Atoms* **2002**, *194*, 1–6. [CrossRef]
46. Olukotun, S.; Mann, K.S.; Gbenu, S.; Ibitoye, F.; Oladejo, O.; Joshi, A.; Tekin, H.; Sayyed, M.; Fasasi, M.; Balogun, F.; et al. Neutron-shielding behaviour investigations of some clay-materials. *Nucl. Eng. Technol.* **2019**, *51*, 1444–1450. [CrossRef]
47. Singh Mann, K. Toolkit for Fast Neutron Removal Cross-Section. In Proceedings of the 3rd International Conference Advancements in Engineering and Technology, Kuantan, Malaysia, 18–19 August 2015; Bhai Gurdas Institute of Engineering and Technology: Punjab, India, 2015.
48. El Abd, A.; Mesbah, G.; Mohammed, N.M.A.; Ellithi, A. A simple Method for Determining the Effective Removal Cross Section for Fast Neutrons. *J. Radiat. Nucl. Appl.* **2017**, *2*, 53–58. [CrossRef]
49. Agostinelli, S.; Allison, J.; Amako, K.; Apostolakis, J.; Araujo, H.; Arce, P.; Asai, M.; Axen, D.; Banerjee, S.; Barrand, G.; et al. Geant4—A simulation toolkit. *Nucl. Instrum. Methods Phys. Res. Sect. A* **2003**, *506*, 250–303. [CrossRef]
50. Hila, F.C.; Asuncion-Astronomo, A.; Dingle, C.A.M.; Jecong, J.F.M.; Javier-Hila, A.M.V.; Gili, M.B.Z.; Balderas, C.V.; Lopez, G.E.P.; Guillermo, N.R.D.; Amorsolo, A.V. EpiXS: A Windows-based program for photon attenuation, dosimetry and shielding based on EPICS2017 (ENDF/B-VIII) and EPDL97 (ENDF/B-VI.8). *Radiat. Phys. Chem.* **2021**, *182*, 109331. [CrossRef]
51. Brun, R.; Rademakers, F. ROOT—An object oriented data analysis framework. *Nucl. Instruments Methods Phys. Res. Sect. A Accel. Spectrometers Detect. Assoc. Equip.* **1997**, *389*, 81–86. [CrossRef]

Disclaimer/Publisher's Note: The statements, opinions and data contained in all publications are solely those of the individual author(s) and contributor(s) and not of MDPI and/or the editor(s). MDPI and/or the editor(s) disclaim responsibility for any injury to people or property resulting from any ideas, methods, instructions or products referred to in the content.